Available online at www.sciencedirect.com
SCIENCE DIRECT®
Catalysis Today 91–92 (2004) 177–180
CATALYSIS TODAY
www.elsevier.com/locate/cattod

# Electronic structure of the extended vanadyl pyrophosphate (1 0 0) surface

D.J. Thompson [a,*], I.M. Ciobîcă [b,1], B.K. Hodnett [a,c], R.A. van Santen [b], M.O. Fanning [a]

[a] *Chemical and Environmental Sciences Department, University of Limerick, Limerick, Ireland*
[b] *Schuit Institute of Catalysis, Eindhoven University of Technology, PO Box 513, 5600 MB Eindhoven, The Netherlands*
[c] *Materials and Surface Science Institute, University of Limerick, Limerick, Ireland*

Available online 24 April 2004

**Abstract**

Bulk and (1 0 0) surface vanadyl pyrophosphate, $(VO)_2P_2O_7$, were analysed via periodic density functional theory calculations. Electronic structures were computed using the Perdew–Wang 91 functional, together with ultrasoft pseudopotentials and plane wave basis sets with cut-off energy of 400 eV. *k*-point sampling was restricted to the centre of the first Brillouin zone. Periodic surface models were built from one bulk unit cell, with the vacuum gap between successive layers made equal to the length of the surface slab in the direction normal to the (1 0 0) plane. Tests indicated that these conditions are sufficient to accurately model surface reactivity. Density of states (DOS) plots show that vanadium species are the primary surface electron transfer sites. Terminal P–O oxygen species are the most basic surface oxygens, as indicated by their strong contribution to high-lying valence band levels. Results for periodic calculations on the $(VO)_2P_2O_7$ (1 0 0) surface are hence qualitatively identical to those previously obtained from cluster calculations, with $(VO)_2P_2O_7$ (1 0 0) vanadium species acting as hydrocarbon chemisorption sites, nucleophilic terminal P–O oxygens performing substrate oxyfunctionalisation to non-combustion products, and protection of the mild oxidation product dependent on its orientation at the surface.


*Keywords:* Vanadyl pyrophosphate; DFT periodic calculations; Hydrocarbon selective oxidation; Density of states

## 1. Introduction

The selective oxidation of *n*-butane to maleic anhydride over vanadyl pyrophosphate, $(VO)_2P_2O_7$, is the most successful industrial alkane oxyfunctionalisation process, with much debate [1–4] regarding catalyst mode of action in *n*-butane activation and mild oxidation. While there exist conflicting reports in the literature (see, for example [5], and references therein) concerning the nature of the working catalyst surface, ab initio electronic structure calculations [6–8] on active site clusters at the crystalline (1 0 0) surface have provided some insights into the selective oxidation mechanism, with the observed [1–4] importance of surface vanadium species and also surface-enrichment in phosphorus rationalised by the high covalent reactivity of vanadium [6,8] and terminal P–O oxygen [8] at the $(VO)_2P_2O_7$ (1 0 0) surface. Modelling of defective active sites [7] too has created a better understanding of the role of oxygen vacancies in surface reactivity. In the present paper, we report a quantum chemical study of the extended (1 0 0) surface. Surface reactivity is analysed using local density of states (DOS) distributions. Characterisation of the surface in terms of local basicity and acidity allows prediction of site-selectivity for substrate chemisorption, while selective oxygen species for hydrocarbon oxyfunctionalisation are identified from examination of high-lying valence band levels.

## 2. Theory and surface model

### 2.1. Computational details

In all calculations, the Perdew–Wang (PW91) exchange-correlation functional [9] was used, together with ultrasoft pseudopotentials [10] and plane wave basis sets with cut-off energy of 400 eV. Bulk and surface electronic structures were computed using VASP [11–13], with CASTEP [14] also used, to calculate bulk bond overlap populations. *k*-point

* Corresponding author.
*E-mail address:* damien.thompson@ul.ie (D.J. Thompson).
[1] Present address: Sasol Technology, Research & Development, Schuit Institute of Catalysis, Eindhoven University of Technology, PO Box 513, 5600 MB Eindhoven, The Netherlands.

0920-5861/$ – see front matter © 2004 Elsevier B.V. All rights reserved.
doi:10.1016/j.cattod.2004.03.030

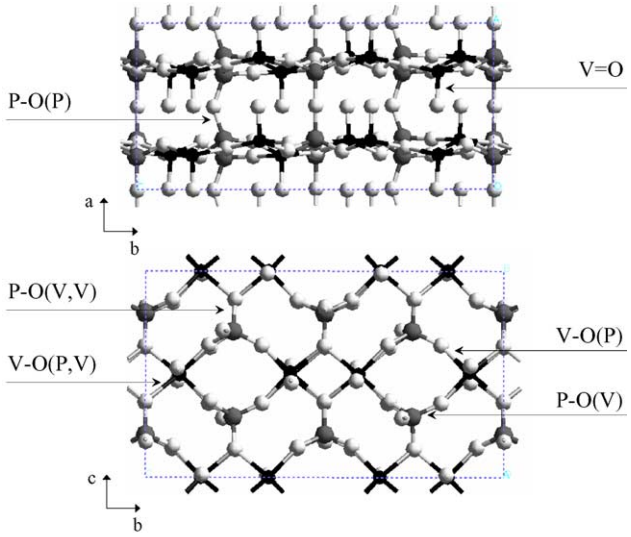


| Bond Type | | Bond Length [16], Å | Mulliken Population, a.u. |
|---|---|---|---|
| V-O(P,V) | 2.0 | 7 | 0.06 |
| V-O(P) | 1.9 | 5 | 0.11 |
| V=O | 1.6 | 0 | 0.45 |
| P-O(P) | 1.5 | 8 | 0.43 |
| P-O(V,V) | 1.5 | 6 | 0.55 |
| P-O(V) | 1.4 | 9 | 0.66 |

Fig. 1. Bonding in bulk $(VO)_2P_2O_7$, projected on to the (0 0 1) and (1 0 0) planes, respectively. Vanadium atoms are coloured black, phosphorus grey and oxygen white. Dashed lines mark unit cell boundaries.

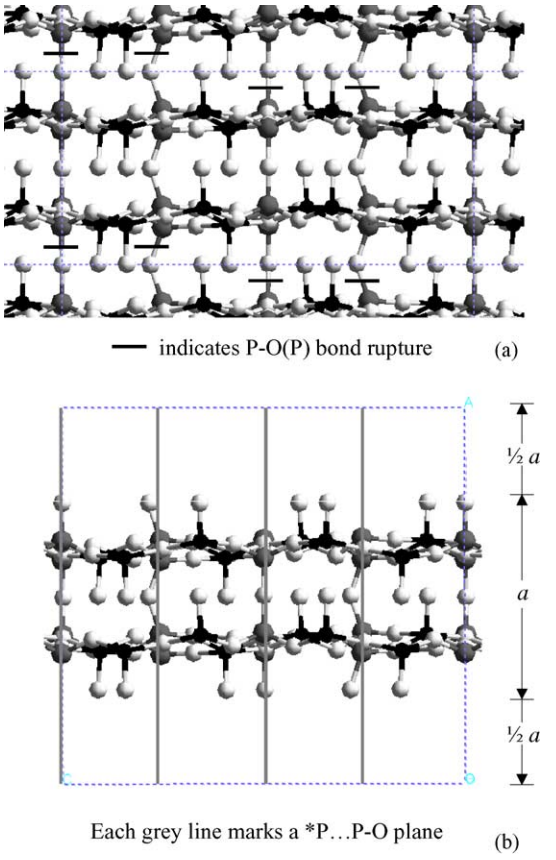


Fig. 2. Generation of the (1 0 0) surface model. See text for details.

sampling was restricted to $\Gamma$, the centre of the first Brillouin zone; bulk and surface calculations with Monkhorst–Pack [15] grids up to $4 \times 4 \times 4$ and $2 \times 2 \times 1$, respectively, yielded electronic properties qualitatively identical to those obtained using $1 \times 1 \times 1$ meshes.

### 2.2. (1 0 0) surface model

#### 2.2.1. Bulk crystal bonding

Fig. 1 shows bond nomenclature, bond lengths [16], and calculated Mulliken bond overlap populations in the bulk $(VO)_2P_2O_7$ crystal lattice.

P–O(V) and P–O(V,V) bonds are stronger than V–O(P) and V–O(P,V) bonds, reflecting the greater atomic electronegativity of P relative to V. Within the [P–O(V), P–O(V,V)] and [V–O(P), V–O(P,V)] pairs, the metal–oxygen bond with oxygen coordinated to one, rather than two, other atoms, is stronger, in agreement with chemical intuition. Bond densities are inversely proportional to bond lengths, except for P–O(P) and V=O; the shorter P–O(P) bond has a lower overlap population, although the difference between the two is slight. Calculations using refined [17] bulk geometry gave qualitatively identical results. Hence, P–O(P) bonds were cleaved for (1 0 0) surface formation. The favourability of P* over V* (1 0 0) surface sites, where $*$ denotes a terminal oxygen vacancy, is in agreement with calculated anion defect stabilities [7].

#### 2.2.2. (1 0 0) surface models

Stoichiometric surface models, based on one bulk unit cell, were cleaved from the experimental [16] bulk crystal structure. Fig. 2 shows how a formally neutral (1 0 0) surface model was cleaved from the bulk.

Bulk bond rupturing for the creation of one possible (1 0 0) surface atomic configuration is shown in Fig. 2(a). A vacuum width equal to the length, *a*, of the surface slab in the direction normal to the (1 0 0) plane, as shown in Fig. 2(b), prevents electronic interaction between slabs. Creation of formally neutral surfaces, under the restriction of generating models featuring one terminal P–O oxygen vacancy along each of the (0 4 0) family of planes marked explicitly in Fig. 2(b), leads to six possible surfaces. Surface geometry shown in Fig. 2(b) corresponds to the surface model featuring the least oxygen–oxygen electrostatic repulsion at each face termination. This model has the lowest calculated creation energy, and is used in subsequent analysis of (1 0 0) surface electronic structure. A surface model twice as large in the direction normal to the (1 0 0) plane gave the same electronic properties.

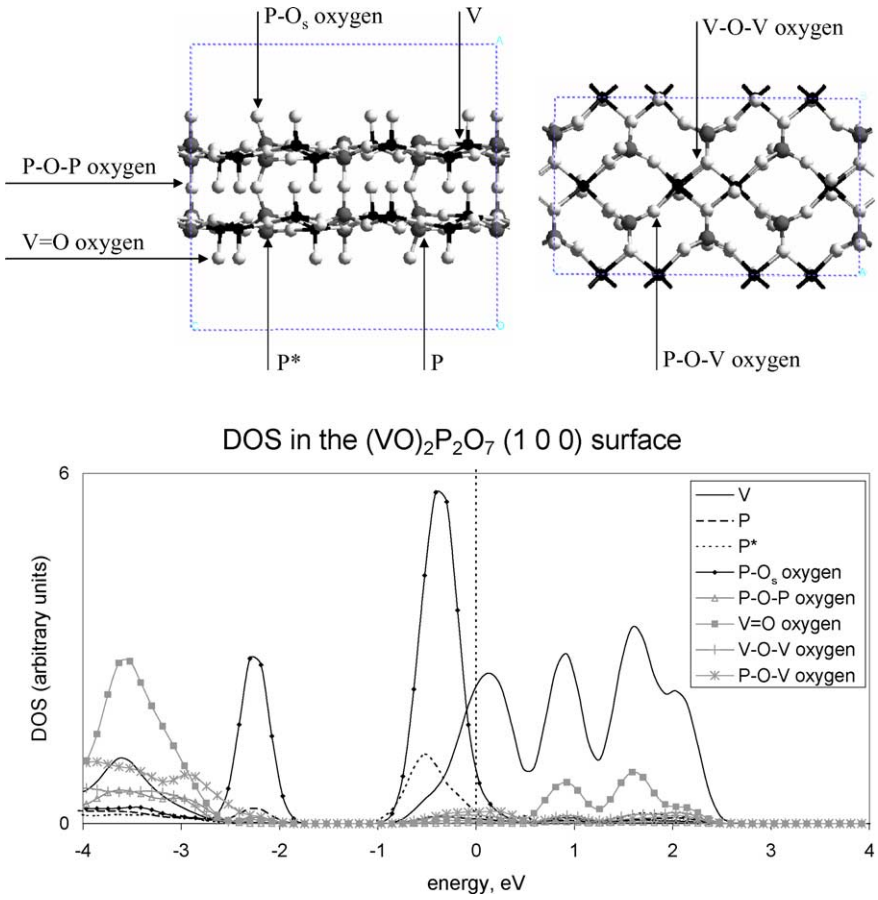


Fig. 3. Local DOS distributions in the $(VO)_2P_2O_7$ (1 0 0) surface. Vanadium atoms are coloured black, phosphorus grey and oxygen white, with the surface model shown in side-on and plan views, respectively. $O_s$ labels terminal P–O oxygen, while $*$ denotes a terminal P–O oxygen vacancy. Dashed lines mark unit cell boundaries. The dotted vertical line in the DOS plot marks $\varepsilon_f$.

## 3. Results and discussion

There are many more electrons involved in solid-state, compared to molecular modelling, making it less meaningful to single out a particular energy level (and corresponding orbital) in analysing the reactivity of a system. So, to recover frontier orbital concepts, one must look at the wavefunction in a particular energy *interval*.

Shown in Fig. 3 are local (per atom, with each distribution summed over s, p and d components) density of states distributions in the energy range −4 to +4 eV for the (1 0 0) surface. Orbital-projected partial density of states (PDOS) distributions, not shown, indicate that, in both bulk and surface structures, the core region is built principally from oxygen s, and metal s and p, orbitals. Oxygen p orbitals predominate all but the outermost valence band levels. Highest occupied and lowest unoccupied energy levels are built from vanadium 3d orbitals, with the Fermi level marking the transition from valence to conduction band regions—the underestimation of valence–conduction band gaps in transition-metal oxides is a systematic error in DFT calculations [18]. Higher-lying virtual levels are also sited principally on vanadium, with a small contribution from vanadium–oxygen combinations, particularly d,p-hybridised V=O, orbitals. Other surface oxygen types do not contribute significantly to conduction band levels.

Local nucleophilicity in the $(VO)_2P_2O_7$ (1 0 0) surface is propagated through vanadium 3d orbitals and then P–$O_s$ oxygen 2p orbitals, with vanadium's large 3d orbital contribution also to the bottom of the conduction band indicating its dual role as surface base and surface acid site. Other surface oxygen species do not contribute significantly to near-Fermi energy levels, indicating that vanadium reactivity is propagated through unhybridised orbitals, i.e., in-phase (frontier occupied) and out-of-phase (frontier unoccupied) combinations of vanadium 3d orbitals. The presence of P–$O_s$ oxygen species in the high-energy region of the valence band indicates their role as nucleophilic oxygens for mild oxidation of hydrocarbon molecules at the $(VO)_2P_2O_7$ (1 0 0) surface. The higher concentration of P–$O_s$ oxygens at a phosphorus-enriched (pyrophosphate-terminated [8,19]) surface active site offers an explanation for the observed [1–4] role of surface-enrichment in phosphorus in promoting the selective oxidation of *n*-butane to maleic anhydride.

The electronic structure of the (1 0 0) surface with super-stoichiometric P/V ratio, as well as treatment of

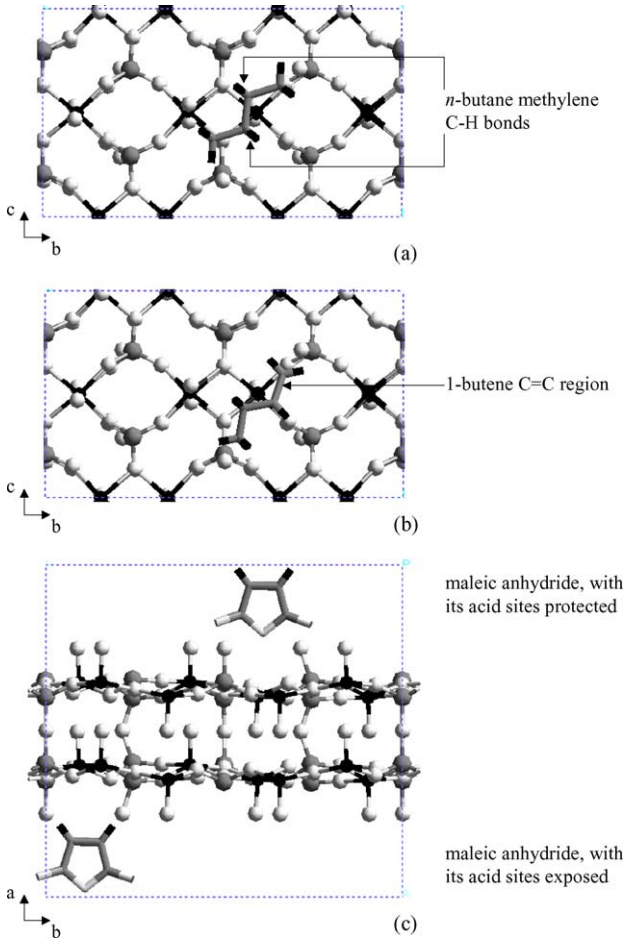


Fig. 4. Substrate chemisorption on $(VO)_2P_2O_7$ (1 0 0). Panels (a) and (b) show, respectively, plan views of *n*-butane and 1-butene at surface vanadium sites. Panel (c) shows a side-on view of maleic anhydride at the surface. Substrate molecules are shown in cylinder representation with carbons grey, hydrogens black and oxygens white. Surface vanadium atoms are coloured black, phosphorus grey and oxygen white.

surface ionic relaxtion and hydration effects, will be published elsewhere [20]. Valence band X-ray photoelectron spectroscopy experiments would also be useful in further characterising vanadyl pyrophosphate surface reactivity.

## 4. Conclusions

Periodic surface calculations support mechanisms previously proposed for *n*-butane [8], 1-butene [21] and maleic anhydride [8] electron transfer with, and hence transformation in, $(VO)_2P_2O_7$ (1 0 0) active site clusters, as illustrated in Fig. 4.

Briefly, *n*-butane methylene carbons donate electron density to surface vanadium species, with contemporaneous base attack by vanadium on methylene hydrogens, in the selective activation of *n*-butane [8]. 1-Butene adsorption involves formation of a strongly-bound π-cation complex at surface vanadium sites [21]. In post-activation oxidative transformation of either the paraffin or olefin substrate, the availability of nucleophilic $P–O_s$ oxygen species determines the selectivity to maleic anhydride. Upon formation in the active site, presuming a hydrocarbon–vanadium chelating configuration [22] in the earlier stages of reaction, highly electronegative maleic anhydride will not be further transformed, due to blocking of its $sp^2$ carbon acid sites from surface base sites. If allowed to re-adsorb following its synthesis, maleic anhydride may be further transformed via nucleophilic attack by surface base sites [8].

## References

[1] G. Centi, F. Trifiro, J.R. Ebner, V.M. Franchetti, Chem. Rev. 88 (1988) 55.
[2] G. Centi, Catal. Today 16 (1993) 1.
[3] J.C. Volta, C.R. Acad, Sci. Ser. IIc: Chim. 3 (2000) 717.
[4] B.K. Hodnett, Heterogeneous Catalytic Oxidation: Fundamental and Technological Aspects of the Selective and Total Oxidation of Organic Compounds, Wiley, 2000.
[5] V.V. Guliants, J.B. Benziger, S. Sundaresan, I.E. Wachs, J.M. Jehng, J.E. Roberts, Catal. Today 28 (1996) 275.
[6] M. Witko, R. Tokarz, J. Haber, K. Hermann, J. Mol. Catal. A: Chem. 166 (2001) 59.
[7] A. Haras, H.A. Duarte, D.R. Salahub, M. Witko, Surf. Sci. 513 (2002) 367.
[8] D.J. Thompson, M.O. Fanning, B.K. Hodnett, J. Mol. Catal. A: Chem. 198 (2003) 125.
[9] J.P. Perdew, J.A. Chevary, S.H. Voskok, K.A. Jackson, M.R. Pederson, D.J. Singh, C. Fiolhais, Phys. Rev. B 46 (1992) 6671.
[10] D. Vanderbilt, Phys. Rev. B 41 (1990) 7892.
[11] G. Kresse, J. Hafner, Phys. Rev. B 47 (1993) 558.
[12] G. Kresse, J. Furthmüller, Phys. Rev. B 54 (1996) 1169.
[13] G. Kresse, J. Furthmüller, Comput. Mater. Sci. 6 (1996) 15.
[14] M.C. Payne, M.P. Teter, D.C. Allan, T.A. Arias, J.D. Joannopoulos, Rev. Mod. Phys. 64 (1992) 1045.
[15] H.J. Monkhorst, J.D. Pack, Phys. Rev. B 13 (1976) 5188.
[16] Y.E. Gorbunova, S.A. Linde, Sov. Phys. Dokl. 24 (1979) 138.
[17] H.J. Koo, M.J. Whangbo, P.D. VerNooy, C.C. Torardi, W.J. Marshall, Inorg. Chem. 41 (2002) 4664.
[18] I. Pollini, A. Mosser, J.C. Parlebas, Phys. Rep. 355 (2001) 1.
[19] J.R. Ebner, M.R. Thompson, Catal. Today 16 (1993) 51.
[20] D.J. Thompson, I.M. Ciobîcã, B.K. Hodnett, R.A. van Santen, M.O. Fanning, Surf. Sci. 547 (2003) 438.
[21] D.J. Thompson, M.O. Fanning, B.K. Hodnett, J. Mol. Catal. A: Chem. 206 (2003) 435.
[22] B. Chen, E.J. Munson, J. Am. Chem. Soc. 124 (2002) 1638.